Journal of Non-Crystalline Solids 358 (2012) 952–958

Contents lists available at SciVerse ScienceDirect

Journal of Non-Crystalline Solids

journal homepage: www.elsevier.com/ locate/ jnoncrysol

Influence of Bi_2O_3 content on the crystallization behavior of TeO_2–Bi_2O_3–ZnO glass system

Xiao Hu [a], Guillaume Guery [a,b], Joshua Boerstler [a], J. David Musgraves [a,*], Don Vanderveer [c], Peter Wachtel [a], Kathleen Richardson [a]

[a] School of Material Science and Engineering, COMSET, Clemson University, Clemson, SC 29634, USA
[b] CNRS, Universite de Bordeaux, ICMCB, 87 av. Dr. A. Schweitzer, Pessac, F-33608, France
[c] Department of Chemistry, Clemson University, USA

ARTICLE INFO

Article history:
Received 29 September 2011
Received in revised form 2 January 2012
Available online 30 January 2012

Keywords:
Tellurite glass ceramic;
Bi_2O_3 content;
Crystallization behavior

ABSTRACT

Glass ceramic materials with composition $75TeO_2$–xBi_2O_3–(25-x)ZnO (x = 13, 12, 11) possessing transparency in the near- and mid-infrared (MIR) regions were studied in this paper. It was found that as the Bi_2O_3 content increased in the glass composition, the observed crystallization tendency is enhanced, and high crystal concentrations were obtained for the glasses with high Bi_2O_3 content while maintaining transparency in the MIR region. Crystal size in the glass ceramic was reduced by adjusting the heat treatment conditions; the smallest average size obtained in this study is 700 nm. $Bi_{0.864}Te_{0.136}O_{1.568}$ was identified using X-ray Diffraction (XRD) and found to be the only crystal phase developed in the glass ceramics when the treatment temperature was fixed at 335 °C. The morphology of the crystals was studied using Scanning Electron Microscopy (SEM), and crystals were found to be polyhedral structures with uniform sizes and a narrow size distribution for a fixed heat treatment regime. Infrared absorption spectra of the resulting glass ceramics were studied. The glass ceramic retained transparency in the infrared region when the crystals inside were smaller than 1 μm, with an absorption coefficient less than 0.5/cm in the infrared region from 1.25 to 2.5 μm. The mechanical properties were also improved after crystallization; the Vickers Hardness value of the glass ceramic increased by 10% relative to the base glass.

1. Introduction

Tellurite glasses have drawn much attention in recent years and are considered as promising materials for a variety of optical devices such as optical switches, fibers and optical storage devices due to their high transmittance from the visible to mid-infrared (MIR) spectral regions, high refractive index (n > 2) and unique non-linear optical properties [1–3].

At the same time, tellurite glass ceramics have also attracted increasing interest; tellurite glass is considered to be a good host-glass matrix in which to form crystalline phases because its high refractive index is close to that of many crystals, and this index match reduces scattering loss at crystal-glass interfaces. The formation of these crystals breaks the long-range average isotropy of the tellurite glass and can lead to high values for non-linear optical properties such as second harmonic generation (SHG) in tellurite glass ceramics [4–6]. Other optical properties such as luminescence or up-conversion in rare earth doped tellurite glass ceramics had also been studied extensively in recent years [7,8]. Additionally, the mechanical properties of the base glass have been demonstrated to improve after crystallization in tellurite glasses such as the BaO–Er_2O_3–TeO_2 system. [9]. Based on these previous research efforts, tellurite glass ceramics show great potential for applications in the field of optical functional devices [10,11].

Recently, it was found that TeO_2–Bi_2O_3–ZnO (TBZ) glasses containing crystal phases exhibited high second harmonic generation and were considered to be promising materials for non linear optical applications [2,12] and the crystallization kinetics and thermal behavior of this glass system have drawn increasing interest with the goal of achieving superior optical properties and functionalities. [13–15].

The TeO_2–Bi_2O_3–ZnO system studied in this paper is based on results demonstrated in some of our earlier work [13]. In the present work, TeO_2, Bi_2O_3 and ZnO contents were varied in order to improve the crystallization behavior exhibited by this glass system. During the experiments, it was found that the crystal concentration was most strongly impacted by changes in the Bi_2O_3 content. Therefore, to examine the influence of Bi_2O_3 content on the crystallization behavior, a composition of $75TeO_2$–xBi_2O_3–(25-x)ZnO was chosen to be studied systematically, where "x" was chosen to be 11, 12 and 13 within the glass forming region. Thermal properties and crystallization behavior were investigated and compared within different compositions and thermal treatments. Infrared absorption spectra and Vickers Hardness of resulting glass ceramics of the composition $75TeO_2$–$13Bi_2O_3$–12ZnO were studied. Heat treatment times were

* Corresponding author.
E-mail address: jdm047@clemson.edu (J.D. Musgraves).

0022-3093/$ – see front matter © 2012 Elsevier B.V. All rights reserved.
doi:10.1016/j.jnoncrysol.2012.01.009

chosen in an attempt to realize glass ceramic morphology possessing small crystallites with narrow crystallite size distributions within the glassy matrix leading to good optical transparency. The resulting glass ceramic was shown to retain transparency in the infrared region when the crystals formed in the host glass are smaller than 1 μm with refractive indices close to that of the parent glass; and the mechanical properties were also modestly improved after crystallization. Enhanced strength, high transmission in the infrared region, and potential optical functions resulting from crystallization and uniform crystal phase make this glass ceramic promising material for various fiber-based applications and other optical communication and storage devices.

2. Experimental

Glasses with composition of $75TeO_2$–xBi_2O_3–(25-x)ZnO (x = 13,12,11) were prepared with high purity raw materials: TeO_2 (Alfa Aesar, Tech, 99.999%), Bi_2O_3 (Alfa Aesar, Tech, 99.999%) and ZnO (Alfa Aesar, Tech, 99.0%). Raw materials (50 g) were mixed and then melted in a platinum crucible at 850 °C for 15 min. The glass melt was then cast on a brass plate which had been pre-heated at 285 °C. The glass then was annealed at 285 °C for 8 h. A two-step heat treatment was used to nucleate and then grow the crystals in glass matrix. Firstly, the base glass was heated at 330 °C for 22 h for nucleation, samples were then heated at 335 °C for either 2, 7, 11, 17, 22, 26, 30 or 64 h to induce varying levels of crystal growth. Following heat treatment, the glass ceramic samples were cut and given an optical polish for further investigation.

All the characteristic temperatures of the base glasses were measured with a Differential Scanning Calorimetry (DSC, TA instruments Inc) at a heating rate of 20 °C/min. The measurement was taken from room temperature to 550 °C.

A Nikon Type 115 polarizing optical microscope was used to investigate the microstructure of glasses and glass ceramics. Bright-field images of the glass-ceramic were recorded by a CCD camera. The boundaries of the crystals on the focal plane were found using a Matlab program, and the areas enclosed by the boundaries were calculated, therefore the volume fraction of the crystals can be estimated from the area fraction of the crystals on the focal plane.

The transmittance of the base glass and the glass ceramics in near infrared region was measured using a Magna-IR 560 Fourier Transformed Infrared Spectrometer (FTIR) from Nicolet. The system was purged with N_2 to remove atmospheric water and CO_2 in the sample chamber. The absorption coefficient in the infrared region was calculated based on the transmittance of the glass and glass ceramic samples by considering the effect of Fresnel reflection at the sample surfaces.

X-ray Diffraction (XRD) measurements were performed on the glass ceramic samples with Cu K_α irradiation (1.540562 Å, Rigaku ULTIMA IV In.) at 40 kV and 40 mA. The XRD patterns were compared with International Centre for Diffraction Data (ICDD) PDF files to identify the crystal phases formed in the glass ceramics.

A Bruker Senterra micro-Raman spectrometer was used to investigate the molecular structure of the glasses. A laser at 532 nm with energy of 10 mW was introduced to a microscope and was focused on the glass sample by the objective. The backward Raman scattered light was collected by the same objective and imaged onto a spectrograph equipped with a cooled CCD camera. Raman spectra in the range of 70 to 800 cm^{-1} were recorded with a resolution of 3–5 cm^{-1}.

Vickers hardness was measured for the base glass and glass ceramics using a DUH-211S dynamic micro hardness tester (Shimadzu) with a Vickers indenter. The force load on the sample surface was 25 g with a loading rate of 7.1 gF/s.

Scanning electron microscopy (SEM, Hitachi, SU-6600) was used to investigate the morphology of the crystalline phase in the glass ceramics. Prior to SEM investigation, the glass ceramic samples were etched in 37% HCl solution for 1 min at room temperature to improve contrast.

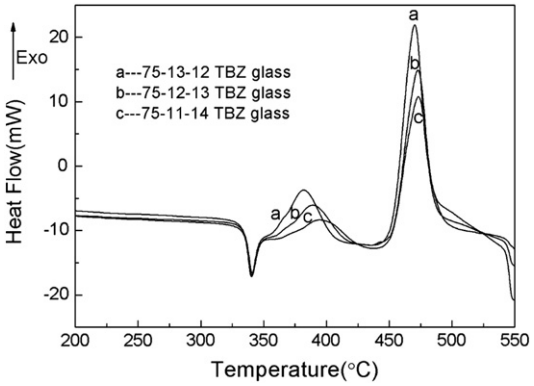

Fig. 1. DSC thermogram of the base glasses in the composition of $75TeO_2$–xBi_2O_3–(25-x)ZnO; x = 11, 12, 13.

3. Results

Characteristic temperatures of the base glasses were obtained from the DSC curves shown in Fig. 1. The glass transition temperature T_g was taken as the inflection point of the endotherm (obtained by taking the first derivative of the curve), the crystallization temperature, T_p, is the maximum of the exothermic peak, and T_x was defined as the onset temperature of the crystallization peak. The characteristic temperatures of the base glasses are shown in Table 1; the accuracy of the measurement is ±2 °C.

As shown in Fig. 1, T_x and T_p decrease when the Bi_2O_3 content is increased in the glass compositions. T_g for the different compositions are the same to within the experimental error of the instrument. The $75TeO_2$–$13Bi_2O_3$–12ZnO glass has the smallest ΔT, which is defined as $(T_{x1} - T_g)$, also known as the crystallization window. In general, a small value of ΔT indicates the instability of the thermal properties of glasses.

Fig. 2 shows microscope images of glass ceramics with different compositions after the same heat treatment. Glasses with different compositions were heated at 330 °C for 22 h for nucleation, then 335 °C for 22 h for crystal growth. Fig. 2(a) shows the glass ceramic with a composition of $75TeO_2$–$13Bi_2O_3$–12ZnO, crystals with uniform size (about 5 μm) were dispersed homogenously in the glass matrix, and the crystal concentration is much higher than that found in the glass ceramics with the compositions of $75TeO_2$–$12Bi_2O_3$–13ZnO and $75TeO_2$–$11Bi_2O_3$–14ZnO which are shown in Fig. 2(b) and (c), respectively. The crystal volume fraction can be estimated from the microscope images using a Matlab program: the area fraction of crystals was calculated for a given focal plane, and the volume fraction was estimated from this value by assuming the presence of uniformly sized and distributed particles in the matrix. For Fig. 2(a), the crystal volume fraction is about 5%, for Fig. 2(b) and (c), the crystal volume fractions are both less than 1%. It was found that when the Bi_2O_3 content was increased in the composition, crystal formation was enhanced dramatically and higher crystal concentration was obtained under the same heat treatment.

Table 1
Characteristic temperatures of the base glasses in the composition of $75TeO_2$–xBi_2O_3–(25-x)ZnO; x = 11, 12, 13.

Characteristic temperature (±2 °C)	T_g	T_{x1}	T_{p1}	T_{x2}	T_{p2}	T_{x3}	T_{p3}	$\Delta T = (T_{x1} - T_g)$
75TeO2–13Bi2O3–12ZnO	333	358	366	368	382	442	470	25
75TeO2–12Bi2O3–13ZnO	333	361	365	376	389	451	473	28
75TeO2–11Bi2O3–14ZnO	335	363	385	381	395	443	473	28

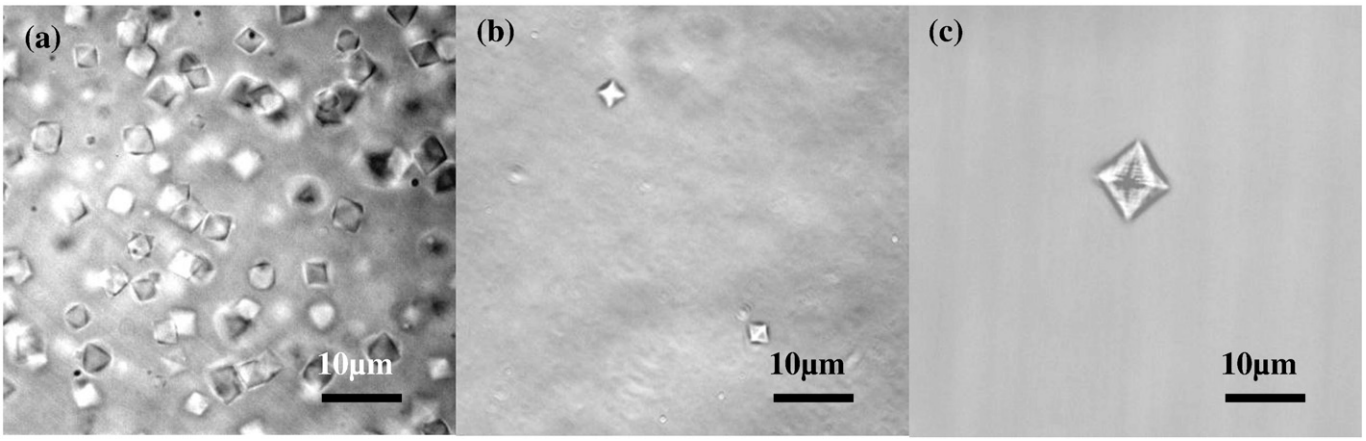

Fig. 2. Optical micrographs (100× objective lens) of TBZ Glass ceramic in the composition of: (a) $75TeO_2$–$13Bi_2O_3$–12ZnO; (b) $75TeO_2$–$12Bi_2O_3$–13ZnO; (c) $75TeO_2$–$11Bi_2O_3$–14ZnO. All the glasses were heated at a nucleation temperature of 330 °C for 22 h, then a subsequent growth step at 335 °C for 22 h.

To analyze the structural mechanisms of the phenomena, the glass structure was investigated using Raman spectroscopy. Laser light of $\lambda = 532$ nm with energy of 10 mW was focused on the base glasses to measure the Raman shift; all the spectra were normalized to the peak located at 740 cm^{-1} which has the highest intensity, the result is shown in Fig. 3.

There are three main bands in the Raman spectra, located at around 400, 650, and 740 cm^{-1}. The peak near 400 cm^{-1} is assigned to the bending mode of O–Te–O linkages; the band near 650 cm^{-1} is attributed to the vibration of the Te–O bonds in the TeO_4 trigonal bipyramid or the Te–O–Te linkages constructed by two unequal Te–O bonds [16,17]; the peak at 740 cm^{-1} is identified as the stretching of Te–O and Te═O which contain non-bridging oxygen in TeO_{3+1} or TeO_3 units. As shown in Fig. 3, the increase of Bi_2O_3 content in the glass composition leads to the intensity increase of bands at 400 cm^{-1} and the decrease of bands at 650 cm^{-1}. In addition, the Raman band at about 400 cm^{-1} is shifted to the lower frequency region as Bi_2O_3 content increased in the composition.

To compare the crystal phases grown in the three glass compositions, the glasses were all heated at 330 °C for 22 h, then 335 °C for 64 h. The XRD patterns were recorded for the three glass ceramics, and the results are shown in Fig. 4. By comparison to XRD patterns in the ICDD data base, the main crystal phase in the $75TeO_2$–$13Bi_2O_3$–12ZnO and $75TeO_2$–$12Bi_2O_3$–12ZnO glass ceramics was identified as $Bi_{0.864}Te_{0.136}O_{1.568}$ with PDF # 38-0865. However, the XRD pattern of the $75TeO_2$–$11Bi_2O_3$–14ZnO does not match this assignment, indicating a different crystal phase or stoichiometry, which has not yet been identified. Future work will explore the evolution (and possible dissolution) of these phases as a function of temperature using hot stage XRD. In Fig. 4, the XRD patterns of glass ceramics in the composition of $75TeO_2$–$12Bi_2O_3$–12ZnO and $75TeO_2$–$11Bi_2O_3$–14ZnO show a broad peak centered at $2\theta = 28°$which represents the base glass, but this peak disappeared in the XRD patterns of the $75TeO_2$–$13Bi_2O_3$–12ZnO glass ceramics. In addition, the intensity of the diffraction peaks of the glass ceramic in $75TeO_2$–$13Bi_2O_3$–12ZnO is much higher than the other two compositions; all of these results indicate the higher relative crystallinity of the glass ceramic in $75TeO_2$–$13Bi_2O_3$–12ZnO [18], this is in agreement with the results of the optical microscopy shown in Fig. 2.

As discussed above, the formation of homogenously dispersed crystals in $75TeO_2$–$13Bi_2O_3$–12ZnO is the best among all of the three glass compositions studied. Low crystallization temperature, high relative crystallinity, and narrow distribution of crystal size make this composition a good choice for high strength glass ceramics. As an important infrared material, transparency in the IR region is always essential for tellurite glass ceramics [3,4,9,16]. Therefore, further work was focused on the optical and mechanical properties of this composition.

With good control of heat treatment, crystal sizes can be reduced and the glass ceramics formed will retain high transparency in the infrared region. Fig. 5 shows SEM images of one of the glass ceramic compositions ($75TeO_2$–$13Bi_2O_3$–12ZnO) which has crystals with sizes ranging from 700 nm to 3 μm depending on the heat treatment used.

To investigate the optical properties of the glass ceramics, samples with thicknesses of 2 mm were optically polished and the transmittance was measured using FTIR. The absorption coefficient α was

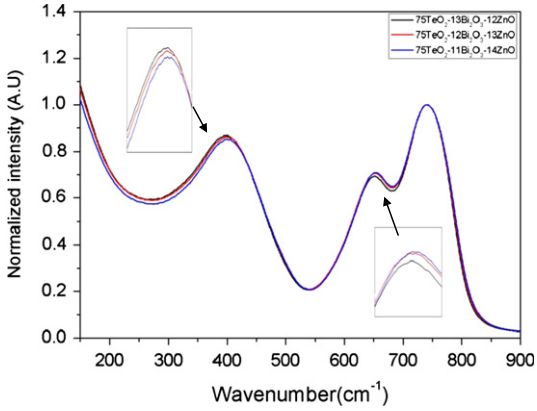

Fig. 3. Raman spectra of glasses in composition of $75TeO_2$–$13Bi_2O_3$–12ZnO, $75TeO_2$–$12Bi_2O_3$–13ZnO and $75TeO_2$–$11Bi_2O_3$–14ZnO. The excitation laser is 532 nm with a power of 10 mW.

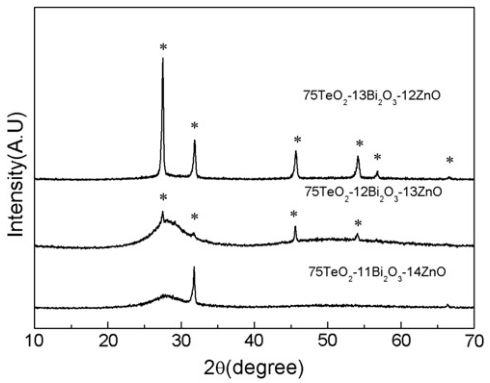

Fig. 4. XRD patterns of glass ceramics in the system of $75TeO_2$–$13Bi_2O_3$–12ZnO, $75TeO_2$–$12Bi_2O_3$–13ZnO and$75TeO_2$–$11Bi_2O_3$–14ZnO. All the glass samples were heated at 330 °C for 22 h, then 335°C for 64 h.* — $Bi_{0.864}Te_{0.136}O_{1.568}$.

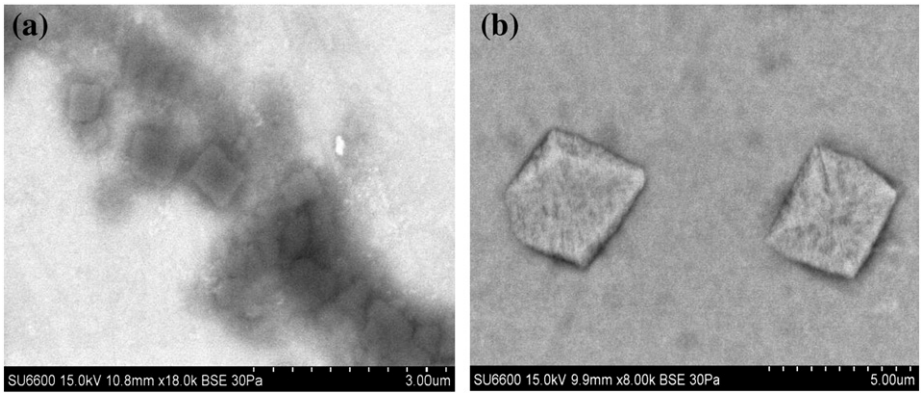

Fig. 5. SEM micrographs of glass ceramics in the composition of $75TeO_2$–$13Bi_2O_3$–12ZnO. (a) Glass was heated at 330 °C for 22 h, then 335 °C for 2 h, crystal size is approximately 700 nm;(b) Glass was heated at 330 °C for 22 h, then 335 °C for 11 h, crystal size is approximately 3 μm; glass ceramics were etched in 37% HCl for 1 min before investigation.

calculated based on the transmittance of glass and glass ceramic samples using the following relations:

$$\alpha = -\frac{1}{t}\ln\frac{T}{(1-R)^2} \quad (1)$$

$$R = \left(\frac{n-1}{n+1}\right)^2 \quad (2)$$

where α is the absorption coefficient of the sample; T is the transmittance; R is the reflection at the sample surfaces; n is the refractive index of the sample; t is the thickness of the sample. As tellurite glasses exhibit high refractive index, the reflection at the surface is typically high and cannot be ignored. Therefore, the absorption coefficient α was calculated considering the reflection of incident light at the sample surfaces as shown in Eq. (1). The absorption coefficient of the base glass and glass ceramics in the $75TeO_2$–$13Bi_2O_3$–12ZnO composition is shown in Fig. 6, where the effective refractive index of the tellurite glass ceramic has been assumed as n = 2.

Glass samples of the $75TeO_2$–$13Bi_2O_3$–12ZnO composition were heated at 335 °C for varying times and the evolved crystal phase was identified using X-ray diffraction for both the glass and glass ceramics, as shown in Fig. 7. This figure shows the XRD patterns of the base glass and glass ceramics, as well as microscope images of glass ceramics as a function of heating time. The XRD patterns were compared with ICDD files to identify the crystalline phases in glass ceramics as $Bi_{0.864}Te_{0.136}O_{1.568}$.

Due to the presence of a single crystal phase, the crystallized volume fraction can be estimated based on the difference in densities between the base glass and the glass ceramics. The density of crystalline

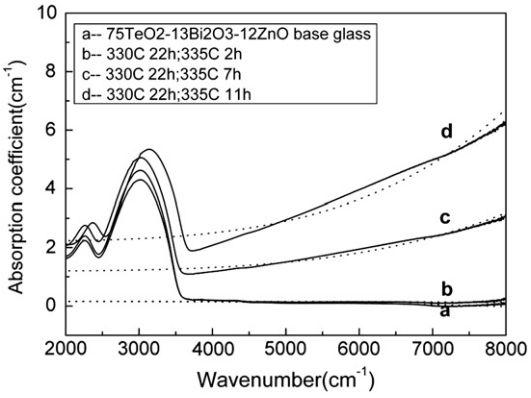

Fig. 6. Absorption coefficient of glass and glass ceramics in the composition of $75TeO_2$–$13Bi_2O_3$–12ZnO, the dotted lines represent fitting curves with the function of λ^{-4}.

$Bi_{0.864}Te_{0.136}O_{1.568}$ is 8.31 g/cm^3 (ICDD), and the density of the base glass of $75TeO_2$–$13Bi_2O_3$–12ZnO was measured to be 6.31 g/cm^3, therefore the crystallized volume fraction can be estimated using Eq. (3):

$$x = \frac{\rho_{gc}-\rho_g}{\rho_c-\rho_g}, \quad (3)$$

where x is the crystallized volume fraction of glass ceramic, ρ_g is the density of base glass (6.31 g/cm^3), ρ_c is the density of crystal (8.31 g/cm^3), ρ_{gc} is the density of glass ceramic measured using Archimedes' principle. The calculated crystallized fraction is shown in Fig. 8; all the glass ceramic were first heated at 330 °C for 22 h for nucleation, then at 335 °C for varying times for crystal growth:

The increase of both crystal size, as estimated from optical microscope images, and Vickers hardness as a function of heat treatment time is shown in Fig. 9.

4. Discussion

An understanding of the crystallization behavior exhibited in this glass system requires an analysis of the mechanism of the influence of Bi_2O_3 content on the crystalization behavior of TBZ glasses. Several physical pathways exist that would describe the increase in the number density of crystals with an increase in Bi_2O_3 content, including an increase in the number of quenched-in nuclei as well as an increase in the tendency for phase separation. Because the glasses were melted under identical conditions, and the distribution of crystals appears uniform throughout the bulk, one explanation of the increase in crystal fraction with increasing Bi content is that the Bi leads to the formation of crystal nuclei in the glass as it is being quenched from the melt. These quenched-in nuclei are extremely difficult to avoid in tellurite glasses, and have been shown to impact the crystallization tendency [3]. In this model, the increased Bi content would induce the formation at high temperatures, close to that of the melt, of Bi-rich crystal nuclei, which are subsequently grown during the thermal treatment. An alternate hypothesis is that the crystallization stability of the high-Bi glasses is reduced due to nanoscale phase separation of a Bi-rich glassy phase in the network. The XRD pattern of the crystallized $75TeO_2$–$13Bi_2O_3$–12ZnO glass in Fig. 4 indicates that the crystalline phase in this glass is $Bi_{0.864}Te_{0.136}O_{1.568}$, which is dramatically richer in Bi than the glass network and would suggest that the crystal nuclei developed during treatment were first formed in the Bi-rich phases in glass. In tellurite glasses with Bi_2O_3 added, some of the Bi^{3+} ions will coordinate non-bridging oxygen and form BiO_6 units or BiO_3 units in the glass matrix [20,21]. When the number of Bi^{3+} ions increases, the number of these units will also increase, which could lead to the formation of a separate Bi-rich phase in the glass matrix. Future work is

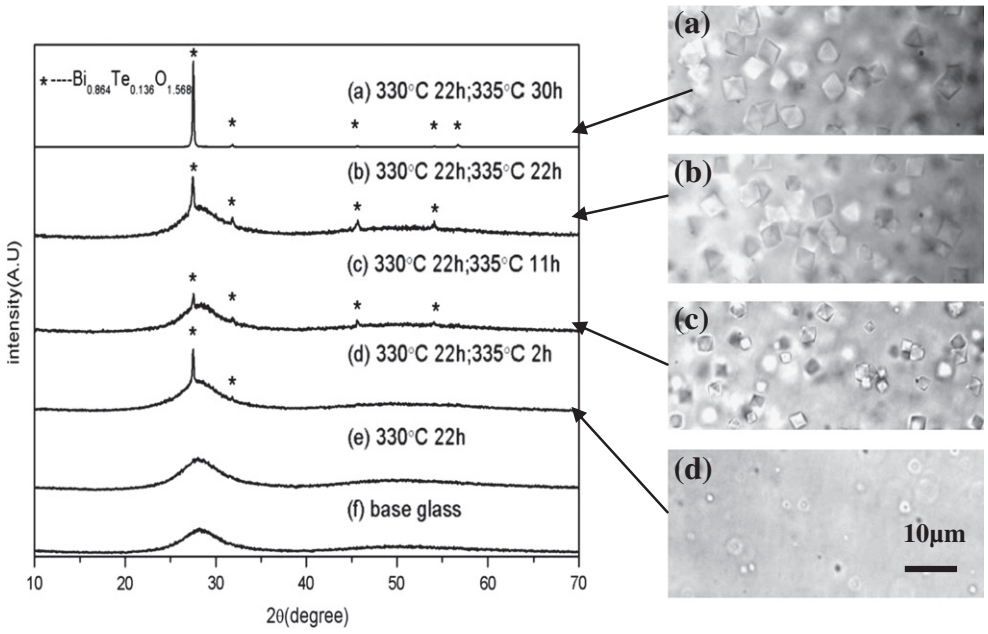

Fig. 7. XRD patterns and optical micrographs (100× magnification) of glass and glass ceramics in the composition space $75TeO_2$–$13Bi_2O_3$–12ZnO for nucleation and growth schedules shown. The microscope images (a), (b), (c) and (d) correspond to the XRD patterns (a), (b), (c) and (d), respectively.

planned using hot stage XRD to study the evolution of these crystal phases in-situ in order to clarify the mechanistic pathways for crystal growth.

To analyze the structural mechanisms of the phenomena, the glass structure was investigated using Raman spectroscopy, which is shown in Fig. 3. The differences, while small due to the minor change in composition, are repeatable and each curve represents the average value of 20 separate measurements. When Bi_2O_3 content increases, the intensity of Raman bands at near 400 cm^{-1} increase while the bands at 650 cm^{-1} decrease; this indicates an increase in the number of O – Te – O linkages and a decrease in the number of TeO_4 units. In addition, the 400 cm^{-1} band is shifted to lower frequency as the Bi_2O_3 content increases, indicating the formation of Te – O – Bi or Bi – O – Bi linkages [16,20]. In tellurite glasses, TeO_4 units are the basic structure units of glass network, and the number decrease of TeO_4 units and replacement of Te – O – Te linkages by the Bi – O – Bi linkages indicates the glass network becomes more open when the Bi_2O_3 content increases, and the appearance of Bi – O – Bi bonds also indicates the formation of BiO_6 groups or BiO_3 groups which can form Bi- rich separate phases easily in the glass [21]. Transportation and aggregation of Bi, Te, and O ions are important processes for the nucleation and growth of $Bi_{0.864}Te_{0.136}O_{1.568}$ crystals, so the rate of nucleation and crystal growth was also influenced by the diffusion rate of atoms when the heating temperature is much lower than the melting temperature [19]. As the free volume of the glass network increases with the addition of Bi_2O_3 and the formation of Bi – O – Bi linkages in the network, the diffusion rate of atoms through the high-Bi_2O_3 glass matrix is expected to be higher at a given temperature, thus leads to higher nucleation and crystal growth rates. In summary, the increase of Bi_2O_3 is shown to enhance the process of nucleation and crystal growth in the glass, and lead to higher crystallinity than the glasses with lower Bi_2O_3 content under the same heating treatment.

As shown in Fig. 5(a) and (b), crystals with uniform size were formed in the glass ceramic. In Fig. 5(a), when the glass was heated at 330 °C for 22 h, then at 335 °C for 2 h, the average crystal size is approximately 700 nm. To get glass ceramics with high transparency, control of the size of the crystals is critical. Forming crystals smaller than the wavelength of the incident light reduces the scattering dramatically, thus increasing the transmission. As an important transparent material in the infrared region, if the crystals in tellurite glass

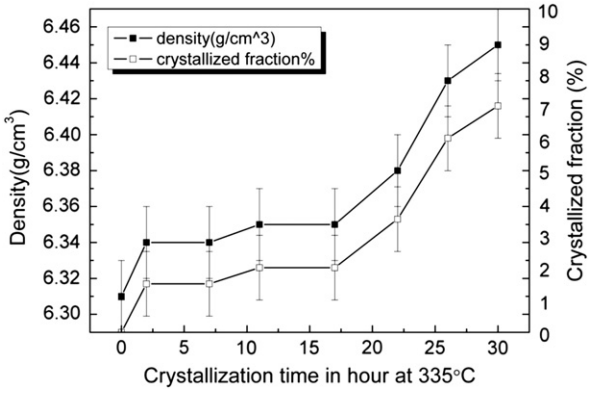

Fig. 8. Density and calculated crystallized volume fraction of glass and glass ceramic in the composition of $75TeO_2$–$13Bi_2O_3$–12ZnO after different heating times (h) at 335 °C for crystal growth. All the glass ceramics were first heated at 330 °C for 22 h for nucleation.

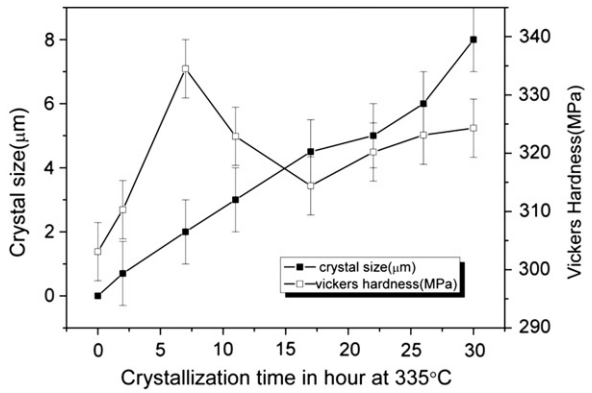

Fig. 9. Crystal size and Vickers hardness of glass ceramics after different crystal growth time. The glass ceramic was firstly heated at 330 °C for 22 h for nucleation. All the glass ceramics are in the composition of $75TeO_2$–$13Bi_2O_3$–12ZnO.

ceramic are less than 1 μm in diameter, scattering of light in the region of interest will be greatly reduced, and the glass ceramic will maintain high transparency in the IR region.

In Fig. 6, curve (b) is the absorption coefficient of the glass ceramic which was heated at 330 °C for 2 h, then 335 °C for 2 h, the absorption coefficient is quite low (<0.5/cm) in the infrared region from 1.25 to 2.5 μm (8000 to 4000 cm^{-1}) and is almost the same as that of the base glass shown in curve (a). As shown in the SEM image in Fig. 5(a), crystal sizes in this glass ceramic are ~700 nm, which is smaller than the wavelength of the infrared light, thus the scattering due to the crystals will be limited during propagation, the absorption will be low and the glass ceramic will retain high transmittance. When the glass was heated at 335 °C for 7 h, as shown in curve (c), the crystal size in the glass reaches ~2 μm, the absorption coefficient in curve (c) is about 4-fold of that in curve (a) in the region from 5000 cm^{-1} (2 μm) to 8000 cm^{-1} (1.25 μm) because the incident light at or below this 2 μm length scale is scattered by the crystals. When the crystal size increased to 3 μm after the sample was heated at 335 °C for 11 h, the absorption coefficient keeps on increasing as shown in curve (d), and is about 10 times of that in curve (a). For all the curves in Fig. 6, the intense absorption band at 3000 cm^{-1} is usually considered to be due to the absorption resonance of the OH group in the glass [3]. It should be pointed out that the absorption coefficient of the glass ceramics is well fit with the function of λ^{-4} from 3600 cm^{-1} to 8000 cm^{-1} (see the dotted fitting lines), suggesting the optical loss in these glass ceramics is mainly due to Rayleigh scattering.

There are no sharp peaks in the XRD spectrum for either the base glass or the glass nucleated at 330 °C for 22 h with no growth treatment, only a broad band centered at $2\theta = 28^{o}$. These samples show no evidence of crystallinity in the XRD. When the glass was then heated at 335 °C for 2 h for crystal growth following the nucleation treatment, as shown in Fig. 7(d), XRD peaks appear indicating the formation of a $Bi_{0.864}Te_{0.136}O_{1.568}$ crystalline phase; the crystal phase did not change when the glass was further heated at the same temperature for 11, 22 and then 30 h, as shown in Fig. 7(a), (b) and (c). Although the crystal size increased as the crystal growth time increased, as shown in the microscope images on the right of Fig. 7, the crystal phase remains the same. Uniform crystal phase makes it easier to estimate and further control the properties of the glass ceramics.

As the heating time increased, both the density of glass ceramics and the crystallized fraction increased progressively. After heating at 330 °C for 22 h, nuclei were already formed in the glass, and when the glass is further heated at 335 °C, a higher temperature for crystallization, larger nuclei will grow while some smaller nuclei will dissolve, and the average crystal size will increase. The crystal fraction will reach 7% when the glass was heated at 335 °C for 30 h. Based on the calculated crystal fraction and crystal size, we can estimate the crystal number density in the glass ceramic. The number densities of glass ceramic with crystallization time of 2, 11, 22 and 30 h are roughly 4.4×10^{16}, 0.25×10^{16}, 0.03×10^{16} and 0.01×10^{16} m^{-3}, respectively. As the growth treatment time increases, the crystal size increases and the number density decreases, indicating that the crystals grow larger due to the dissolution of smaller crystals.

As shown in Fig. 9, the average crystal size in the glass ceramic increased progressively from 700 nm to 8 μm when the crystallization time increased from 2 h to 30 h. Vickers Hardness was also increased initially as a function of crystallization time, but showed a maximum when the crystal size reached 2 μm, after which the hardness decreased to a lower level. A well accepted explanation for this phenomenon is that when the glass is heated at the crystallization temperature for a long time, the thermal mismatch between glass and the crystals evolved in the matrix, along with the increasing crystal volume fraction produces micro-cracks at the crystal-glass interface and reduces the strength of the glass ceramics [22]. To analyze this process, a further study on the microstructure of crystals and fractures is needed.

5. Conclusion

Tellurite glass ceramics in the TeO_2–Bi_2O_3–ZnO system were prepared that exhibited transparency in MIR region. This is believed to be due to the low scatter loss induced by the close refractive index of the resulting crystalline phase as compared to that of the parent glass. The influence of Bi_2O_3 content on the crystallization behavior of this glass system was investigated, and it was found that the increase of Bi_2O_3 content lead to a similar increase of the crystal concentration under the same heat treatment. The mechanism of crystal growth was studied from DSC thermograms and Raman spectra of glasses with differing Bi_2O_3 content. Lastly, Vicker's hardness data for base glass and crystallized glass ceramics showed enhanced mechanical properties of glass ceramics (up to a 10% increase) to that of the parent glass material, suggesting a means whereby the often limited mechanical robustness of tellurite glass and fibers, can be improved.

Acknowledgment

This work was supported in part by the NSF — MWN program (# DMR-0807016).

References

[1] Katsuhisa Tanaka, Aiko Narazaki, et al., Optical second harmonic generation in poled MgO–ZnO–TeO_2 and B_2O_3–TeO_2 glasses, J. Non-Cryst. Solids 203 (1996) 49.
[2] G. Senthil Murugan, E. Fargin, et al., Temperature assisted electrical poling of TeO_2–Bi_2O_3–ZnO glasses for non linear optical applications, J. Non-Cryst. Solids 344 (2004) 158.
[3] Jonathan Massera, "Nucleation and Growth of Tellurite based glasses suitable for Mid-Infrared Application", PhD dissertation, Clemson University, US (2009).
[4] Kazuhide Shioya, Takayuki Komatsu, Hyun Gyu Kim, et al., Optical properties of transparent glass ceramics in K2O–Nb2O5–TeO2 glasses, J. Non-Cryst. Solids 189 (1995) 16–24.
[5] M. Niyaz Ahamad, A. Vasudevarao, et al., Temperature dependent blue second harmonic generation in Ba5Li2Ti2Nb8O30 microcrystals embedded in TeO2 glass matrix, J. Non-Cryst. Solids 355 (2009) 1517.
[6] Ryosuke Sakai, Yasuhiko Benino, Takayuki Komatsu, Enhanced second harmonic generation at surface in transparent nanocrystalline TeO2-based glass ceramics, Appl. Phys. Lett. 77 (2000) 2118–2120.
[7] K. Hirano, Y. Benino, T. Komatsu, Rare earth doping into optical nonlinear nanocrystalline phase in transparent TeO_2-based glass ceramics, J. Phys. Chem. Solids 62 (2001) 2075–2082.
[8] S.K. Singh, N.K. Giri, et al., Enhanced upconversion emission in Er3+-doped tellurite glass containing silver nanoparticles, Solid State Sci. 12 (2010) 1480–1483.
[9] K. Narita, Y. Benino, T. Fujiwara, T. Komatsu, Vickers nanoindentation hardness and deformation energy of transparent erbium tellurite nanocrystallized glasses, J. Non-Cryst. Solids 316 (2003) 407–412.
[10] T.M. Monro, H. Ebendorff-Heidepriem, et al., Emerging nonlinear optical fibers: revised fundamentals, fabrication, and access to extreme nonlinearity, IEEE J. Quantum Electron. 45 (2009) 1357–1364.
[11] D. Buccoliero, H. Steffensen, O. Bang, H. Ebendorff-Heidepriem, T.M. Monro, Thulium pumped high power supercontinuum in loss-determined optimum lengths of tellurite photonic crystal fiber, Appl. Phys. Lett. 97 (2010) 061106.
[12] E. Yousef, M. Hotzel, C. Rüssel, Effect of ZnO and Bi2O3 addition on linear and non-linear optical properties of tellurite glasses, J. Non-Cryst. Solids 353 (2007) 333–338.
[13] Xiao Hu, Guillaume Guery, J. David Musgraves, Don VanDerveer, Joshua Boerstler, Nathan Carlie, Peter Wachtel, Simon Raffy, Roger Stolen, Kathleen Richardson, Processing and characterization of transparent TeO2–Bi2O3–ZnO glass ceramics, J. Non-Cryst. Solids 357 (2011) 3648–3653.
[14] J. Massera, J. Remond, J. Musgraves, M.J. Davis, S. Misture, L. Petit, K. Richardson, Nucleation and growth behavior of glasses in the TeO_2–Bi_2O_3–ZnO glass system, J. Non-Cryst. Solids 356 (2010) 2947–2955.
[15] Abdeslam Chagraoui, Abderrahim Chakib, Adil Mandil, et al., New investigation within ZnO–TeO2–Bi2O3 system in air, Scr. Mater. 56 (2007) 93–96.
[16] J. Ozdanova, H. Ticha, L. Tichy, Remark on the optical gap in ZnO–Bi_2O_3–TeO_2 glasses, J. Non-Cryst. Solids 353 (2007) 2799–2802.
[17] Rajan Jose, Yusuke Arai, Yasutake Ohishi, Raman scattering characteristics of the TBSN-based tellurite glass system as a new raman gain medium, J. Opt. Soc. Am. B 24 (2007) 1517–1526.

[18] John D. Millian, Brian D. Bornhold, Peak height versus peak intensity analysis of X-ray diffraction data, Sedimentology 20 (1973) 445–448.
[19] Robert H. Doremus, Glass Science, 2nd edition John Wiley & Sons, 1994.
[20] A.A. Ali, M.H. Shaaban, Electrical conductivity of silver bismuth borate tellurite glasses, Physica B 403 (2008) 2461–2467.
[21] L. Baia, R. Stefan, W. Kiefer, et al., Structural investigations of copper doped B2O3–Bi2O3 glasses with high bismuth oxide content, J. Non-Cryst. Solids 303 (2002) 379.
[22] P. Hing, P.W. Mcmillan, The strength and fracture properties of glass ceramics, J. Mater. Sci. 8 (1973) 1041–1048.